The Gγ/T-15 Transgenic Mouse Model of Androgen-independent Prostate Cancer: Target Cells of Carcinogenesis and the Effect of the Vitamin D Analogue EB 1089[1]

Carlos M. Perez-Stable,[2] Gary G. Schwartz, Adan Farinas, Milton Finegold, Lise Binderup, Guy A. Howard, and Bernard A. Roos

Geriatric Research, Education, and Clinical Center and Research Service, Veterans Affairs Medical Center, Miami, Florida 33125 [C. M. P-S., A. F., G. A. H., B. A. R.]; Departments of Medicine [C. M. P-S., G. A. H., B. A. R.], Biochemistry and Molecular Biology [G. A. H.], and Neurology [B. A. R.] and Sylvester Comprehensive Cancer Center [C. M. P-S., G. A. H., B. A. R.], University of Miami School of Medicine, Miami Florida 33101; Department of Cancer Biology, Wake Forest University School of Medicine, Winston-Salem, North Carolina 27157 [G. G. S.]; Texas Children's Hospital, Houston, Texas 77030 (M. F.); and Leo Pharmaceuticals, Ballerup, Denmark [L. B.]

Abstract

Transgenic mouse models of prostate cancer provide unique opportunities to understand the molecular events in prostate carcinogenesis and for the preclinical testing of new therapies. We studied the Gγ T-15 transgenic mouse line, which contains the human fetal globin promoter linked to SV40 T antigen (Tag) and which develops androgen-independent prostate cancer. Using the immunohistochemistry of normal mouse prostates before tumor formation, we showed that the target cells of carcinogenesis in Gγ T-15 mice are located in the basal epithelial layer. We tested the efficacy of the $1,25(OH)_2D_3$ analogue, EB 1089, to chemoprevent prostate cancer in these transgenic mice. Compared with treatment with placebo, treatment with EB 1089 at three different time points before the onset of prostate tumors in mice did not prevent or delay tumor onset. However, EB 1089 significantly inhibited prostate tumor growth. At the highest dose, EB1089 inhibited prostate tumor growth by 60% ($P = 0.0003$) and the growth in the number of metastases, although this dose also caused significant hypercalcemia and weight loss. We conducted several *in vitro* experiments to explore why EB 1089 did not prevent the occurrence of the primary tumors. EB1089 significantly inhibited the growth of a Tag-expressing human prostate epithelial cell line, BPH-1, and an androgen-insensitive subline of LNCaP cells [which was not inhibited by $1,25(OH)_2D_3$]. Thus, neither Tag expression nor androgen insensitivity explain the absence of chemopreventive effect. Conversely, neither $1,25(OH)_2D_3$ nor EB 1089 inhibited the growth of the normal rat prostate basal epithelial cell line NRP-152. It is likely that EB 1089 was not effective in delaying the growth of the primary tumor in Gγ T-15 transgenic mice because the target cells of carcinogenesis in these mice are located in the basal epithelial layer. We conclude that Gγ T-15 transgenic mice are a useful model for testing vitamin D-based therapies in androgen-insensitive prostate cancer but are not suitable for studies of vitamin D-based chemoprevention. The superiority of EB 1089 over $1,25(OH)_2D_3$ in the growth suppression of androgen-insensitive prostate cancer cells supports the use of EB 1089 in androgen-insensitive prostate cancer.

Introduction

AIPC[3] is the second leading cause of cancer death in American men (1). Men with cancer that has spread beyond the prostate typically undergo androgen deprivation for palliation. However, the average duration of response to androgen deprivation is only 2 years, and there are no effective therapies for androgen-independent disease (2). Thus, effective treatments for AIPC are urgently needed.

In addition to their responsiveness to androgens, prostate cancer cells respond to another member of the steroid hormone superfamily, $1,25(OH)_2D_3$ (calcitriol). The therapeutic use of vitamin D metabolites is supported by epidemiological studies that first suggested that $1,25(OH)_2D_3$ maintains the differentiated phenotype of prostate cells and that reduced serum levels of $1,25(OH)_2D_3$ or its precursor, 25-hydroxyvitamin D_3, permits the progression of preclinical prostate cancer to clinical disease (3–6). VDR is expressed in most prostate cancer cell lines, and high levels are necessary to mediate the antiproliferative effects *in vitro* (7). However, factors other than VDR density are also important in mediating the antiproliferative effect. For example, the androgen-dependent cell line LNCaP is more sensitive to $1,25(OH)_2D_3$ compared with the androgen-independent PC-3 and DU 145 prostate cancer cell lines, and these differences are not solely attributable to differences in VDR levels (8).

A Phase II clinical trial in AIPC showed that $1,25(OH)_2D_3$

Received 10/12/01; revised 2/22/02; accepted 3/30/02.
The costs of publication of this article were defrayed in part by the payment of page charges. This article must therefore be hereby marked *advertisement* in accordance with 18 U.S.C. Section 1734 solely to indicate this fact.
[1] Supported by Veterans Affairs (VA) Merit Review Entry Program Grant 98-69-01 (to C. M. P-S.), by Grant R01 CA 68565 (to G. G. S.), by Department of Defense Grant DAMD-17-98-1-8525 (to B. A. R.), and by the VA Medical Research Service. G. A. H. has a Senior Research Career Scientist award from the Department of Veterans Affairs.
[2] To whom requests for reprints should be addressed, at Veterans Affairs Medical Center, GRECC (11-GRC), 1201 NW 16 Street, Miami, FL 33125. Phone: (305) 324-4455, extension 4391; Fax: (305) 324-3365; E-mail: cperez@med.miami.edu.

[3] The abbreviations used are: AIPC, androgen-independent prostate cancer; $1,25(OH)_2D_3$, 1,25-dihydroxyvitamin D_3; VDR, vitamin D receptor; PSA, prostate-specific antigen; Tag, (SV40) T antigen; RPA, RNase protection assay; AR, androgen receptor; FBS, fetal bovine serum; PIN, prostate intraepithelial neoplasia; RT-PCR, reverse transcription-PCR; BPH, benign prostatic hyperplasia; TRAMP, transgenic adenocarcinoma mouse prostate; GAPDH, glyceraldehyde 3-phosphate dehydrogenase.

could lower serum PSA levels in some men (9). However, treatment with $1,25(OH)_2D_3$ causes significant hypercalcemia and/or hypercalciurea (10). Synthetic analogues of $1,25(OH)_2D_3$, such as EB 1089 (Seocalcitol; Ref. 11), with potent antiproliferative effects but reduced calcemic effects, can inhibit androgen-independent PC-3 prostate cancer cells *in vitro* (12, 13). EB 1089, acting through VDR, has a cell growth-inhibition mechanism similar to that of $1,25(OH)_2D_3$, but with longer lasting and stronger effects. In LNCaP cells, EB 1089 inhibits the growth of prostate cancer cells by inducing G_1 cell cycle block *in vitro* and has been shown to inhibit tumor growth *in vivo* without producing hypercalcemia (14, 15). In addition, a recent comparison of EB 1089 and $1,25(OH)_2D_3$ treatment in the MATLyLu model of advanced AIPC showed that EB 1089 was as effective as $1,25(OH)_2D_3$ in inhibiting metastases but was significantly less calcemic (16). These results suggest that EB 1089 may offer a therapeutic option in AIPC.

In addition to its therapeutic uses, vitamin D and its analogues may be candidates for use in prostate cancer chemoprevention (17). The rationale for the use of vitamin D metabolites in chemoprevention is that vitamin D may maintain the differentiated phenotype of prostatic cells and delay or reverse the carcinogenic process before invasion and metastasis occur (5, 18). Testing these hypotheses in animals ideally requires models in which the cancer originates from normal prostate epithelial cells in their natural microenvironment and progresses through multiple stages, similar to human prostate cancer (19, 20). One study using the Lobound-Wistar rat model of urogenital cancer showed that treatment with the less calcemic $1,25(OH)_2D_3$ analogue Ro24-5531 resulted in a limited chemoprevention effect (21).

Recently, the advent of several transgenic mouse models of prostate cancer that target the expression of SV40 Tag to specific prostate epithelial cells have provided more suitable systems to test the chemoprevention and therapeutic potential of drugs (20, 22). The present study used Gγ/T-15 transgenic mice (23, 24) to test the efficacy of EB 1089 in the prevention of tumor onset and in the growth inhibition of AIPC. Unlike transgenic models using prostate-specific promoters to target Tag to the prostate epithelial cells, the Gγ/T-15 transgenic mice use the fetal Gγ-globin gene promoter (25). The progression of prostate cancer in 75% of the transgenic males has important similarities to the progression of prostate cancer in men, *e.g.*, originating from high-grade PIN s and progressing to advanced metastatic carcinomas. These tumors are clearly androgen-independent because castration of transgenic males before prostate tumor formation still results in the development of prostate tumors (24). Although Tag is not the cause of prostate cancer in men, the Gγ/T-15 transgenic mice serve as a model of an aggressive, highly metastatic form of AIPC, which is the cause of virtually all deaths from prostate cancer in men.

Materials and Methods

Reagents. EB 1089 was synthesized by Leo Pharmaceuticals (Ballerup, Denmark). EB 1089 was used as a stock solution of 100 mg/ml in Solutol H15 (10 mg/ml), 7.7 mg/ml sodium phosphate dibasic anhydrous, 1 mg/ml sodium phosphate monobasic anhydrous, 2.8 mg/ml sodium chloride, and 10 mg/ml sodium ascorbate and was stored in the dark at 4°C. $1,25(OH)_2D_3$, obtained from Biomol (Plymouth Meeting, PA), was dissolved in ethanol and stored in the dark at −20°C.

Immunohistochemistry. Our previous results showed that the onset of prostate tumors in Gγ/T-15 transgenic mice occurs between 16 and 32 weeks of age (24). To identify the target cells of carcinogenesis, prostates from Gγ/T-15 transgenic mice (14–32 weeks old; $n = 10$) without palpable or visible tumors were removed at necropsy, fixed in 10% buffered formalin for 6 h, dehydrated, embedded in paraffin, and sectioned at 5 μm. Immunostaining for Tag was performed as described previously (26) using a 1:100 dilution of rabbit polyclonal antibody to Tag. The secondary antibody was a biotinylated goat anti-rabbit IgG. Specific color was developed with the Vector ABC kit (Zymed Laboratories Inc., South San Francisco, CA) and enhanced with 3,3′-diaminobenzidine (DAB)-nickel chloride; the sections were counterstained with nuclear Fast Red.

Treatment of Gγ/T-15 Transgenic Males with EB 1089. We used the Gγ/T-15 transgenic mouse model of AIPC (23, 24) to assess the *in vivo* antitumor effect of EB 1089. These mice began to develop prostate tumors by 16 weeks of age (24). At 11 weeks, three of four transgenic males expressed Tag mRNA in the prostate as determined by RPA (data not shown). For this reason, we chose three different treatment starting time points (14, 11, and 9 weeks) before tumor onset to test the ability of EB 1089 to chemoprevent prostate tumors. Transgenic mice (CBA × C57) were identified by DNA slot blot analysis as described previously (24). Transgenic male mice (14, 11, and 9 weeks of age) without palpable tumors were randomly divided into experimental and control groups and were given injections i.p. three times a week with 0.1 ml of freshly prepared EB 1089 at doses of 0.5, 2, 3, 4, 5, and 10 μg/kg body weight (BW) diluted in Solutol H15 or placebo control (Solutol H15). Mice were kept in a 12-hour day/night cycle and fed a normal rodent diet containing 0.95% calcium and 4.5 IU/g vitamin D_3 (Laboratory Rodent Diet 5001; PMI Nutrition International, Purina Mills, Inc., Richmond, IN). Starting at 16 weeks, mice were palpated in the urogenital area 3 days a week to detect prostate tumor mass. End points were 21 days after palpable prostate tumor mass was first detected or at 24 weeks of age. The percentage of mice that developed prostate tumors by 24 weeks of age and the average age when tumors were first detected by palpation (age of onset) were determined for each EB 1089 dose group at 14, 11, and 9 weeks and compared with placebo controls. Mice without a palpable prostate tumor at the 24-week end point but with a visible tumor nodule on dissection of the prostate (usually weighing 25–100 mg) were considered positive for prostate tumor formation. All of the animal studies were carried out with the approval of the Institutional Animal Care and Use Committee at the Miami Veterans Affairs Medical Center (American Association for Accreditation of Laboratory Animal Care-accredited) and conducted in accordance with the NIH Guidelines for the Care and Use of Laboratory Animals.

Prostate Tumor Weight, Serum Calcium, and Body Weight. Twenty-one days after prostate tumors were first detected by palpation, EB 1089- and placebo-treated mice were anesthetized, their blood was collected by cardiac puncture and centrifuged, and the sera were frozen and stored at −80°C. Primary prostate tumors and visible metastases to lymph nodes, adrenal glands, or kidney were removed, and their wet weights determined. Serum calcium was measured by dry slide technology on an automated Kodak Ektachem 700XR clinical chemistry analyzer (Rochester, NY). The body weight for EB 1089-treated and placebo-treated mice was determined at the end of the study. Statistical differences in the wet weights of primary tumor and total metastases, serum calcium, and final body weight between EB 1089- and placebo-treated mice were determined using the two-tailed Student's *t* test.

VDR mRNA Expression by RT-PCR and RPA. RNA from mouse prostate, kidney, and Gγ/T-15 prostate tumor tissue was

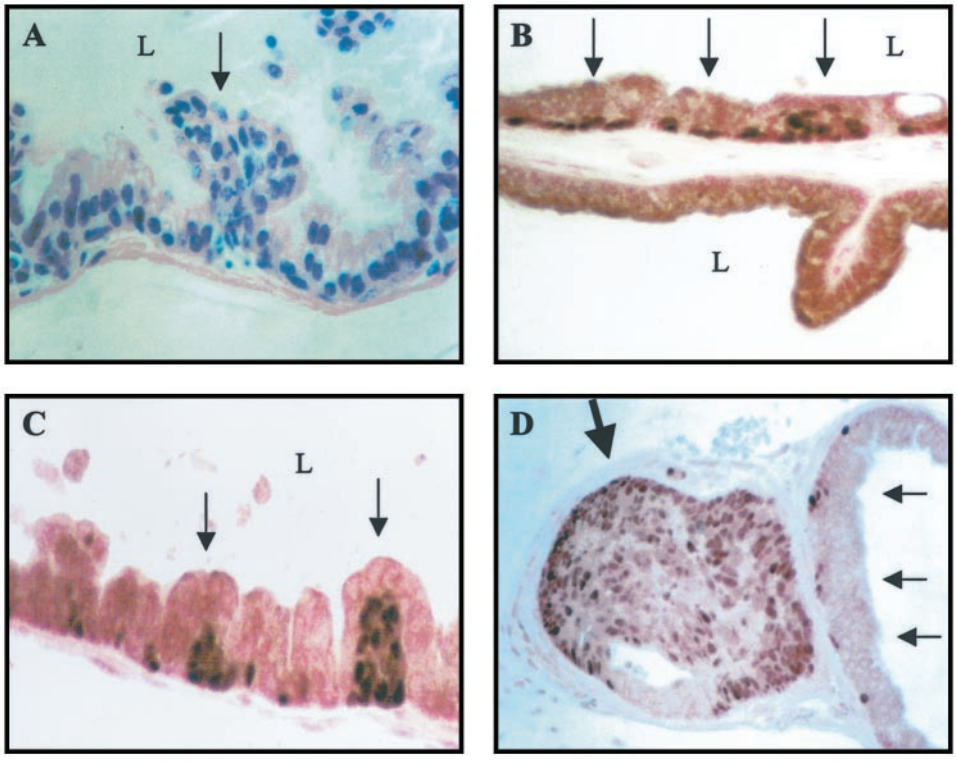

Fig. 1. Prostatic target cells of carcinogenesis in Gγ/T-15 transgenic mice. *A*, light micrograph (H&E, ×400) of preneoplastic lesion similar to high-grade PIN (*arrow*) containing epithelial cells protruding into the lumen (*L*). *B*, light micrograph (nuclear Fast Red, ×200) of Tag immunohistochemistry showing a normal-appearing prostate acini containing Tag-expressing epithelial cells located in the basal epithelial layer (*arrows pointing to cells that contain black nucleus*) next to an acini not containing Tag-expressing cells. *C*, light micrograph (nuclear Fast Red, ×200) showing proliferating Tag-expressing cells (*arrows*) producing an elevation toward the surface layer into the lumen (*L*) of prostate gland. *D*, light micrograph (nuclear Fast Red, ×200) showing prostate duct filled with Tag-expressing dysplastic cells (*large arrow*) next to a normal-appearing prostate duct containing Tag-expressing epithelial cells in the basal layer (*small arrows*).

isolated by the LiCl-urea method (27) and treated with RNase-free DNase. The following DNA oligonucleotides synthesized by Operon Technologies (Alameda, CA) were used for RT-PCR to detect VDR mRNA in mouse prostate and Gγ/T-15 prostate tumor RNA: forward, 5′-GAGTTCTTTTGGTTG-GACA-3′; reverse, 5′-CAGCCTTCACAGGTCATA-3′ (28). Conditions for RT-PCR were: 2 min at 94°C for 1 cycle; 1 min at 94°C, 1 min at 55°C, and 2 min at 72°C for 35 cycles; and 7 min at 72°C for 1 cycle. The expected 209-bp fragment from mouse prostate was cloned into the TA vector pCRII (Invitrogen, Carlsbad, CA), and its identity was confirmed by DNA sequencing. VDR mRNA in mouse kidney, prostate, and Gγ/T-15 prostate tumor was measured by RPA with ^{32}P-labeled Sp6 polymerase-synthesized antisense RNA probe from *Eco*RV-digested mouse VDR/PCRII DNA, using conditions described previously (23).

VDR and AR Western Blot Analysis. Nuclear extracts from mouse (C57) prostate and kidney and from Gγ/T-15 prostate tumors were prepared according to the procedure of Dent and Latchman (29), and protein concentrations were determined with the Bio-Rad protein assay (Bio-Rad Laboratories, Hercules, CA). After the separation of 10 μg of protein by SDS-PAGE, proteins were transferred by electrophoresis to Immobilon-P membrane (Millipore Corp., Bedford, MA) and incubated in 5% nonfat dry milk, PBS, and 0.25% Tween 20 for 1 h. Rabbit polyclonal antibodies specific for VDR (1:1000 dilution, C-20; Santa Cruz Biotechnology, Santa Cruz, CA) and AR (1:1000 dilution., N-20; Santa Cruz Biotechnology) were diluted in 5% nonfat dry milk, PBS, and 0.25% Tween 20 and incubated overnight at 4°C. Membranes were washed in PBS and 0.25% Tween 20 (three times, 10 min each time) and incubated with horseradish peroxidase-conjugated secondary antibody (antirabbit 1:2000 dilution; Santa Cruz Biotechnology) for 1 h, washed in PBS and 0.25% Tween 20, and analyzed by exposure to X-ray film (X-Omat, Eastman Kodak Co., Rochester, NY) using enhanced chemiluminescence plus (ECL plus; Amersham Pharmacia Biotech, Arlington Heights, IL).

Cell Culture and Treatment with 1,25(OH)$_2$D$_3$ and EB 1089. LNCaP-AI is an androgen-independent derivative of the human prostate cancer cell line LNCaP-FGC (Ref. 30; American Type Culture Collection, Manassas, VA), which was spontaneously derived in our laboratory. These cells express AR and PSA, similar to LNCaP-FGC (data not shown). LNCaP-AI cells were maintained in RPMI 1640 (Life Technologies, Inc.) with 5% FBS (Hyclone, Logan, UT), 100 units/ml penicillin, 100 μg/ml streptomycin, and 0.25 μg/ml amphotericin (Life Technologies, Inc.). Unlike androgen-dependent LNCaP-FGC, the LNCaP-AI cells are able to grow long-term in RPMI 1640 with 5% charcoal-stripped FBS (Hyclone) and are referred to as LNCaP-AI/CSS. The Tag-expressing human prostate epithelial cell line BPH-1, generously provided by S. Hayward, was maintained in RPMI 1640 with 5% FBS (31). The normal rat prostate basal epithelial cell line NRP-152, generously provided by D. Danielpour, was maintained in HEPES-free DMEM/F12 (1:1, v/v; Life Technologies, Inc.) with 5% FBS, antibiotic/antimycotic, 20 ng/ml epidermal growth factor, 10 ng/ml cholera toxin, 5 μg/ml insulin (Life Technologies, Inc.), and 0.1 μM dexamethasone (Sigma, St. Louis, MO; Ref. 32).

To determine and compare prostate cell growth inhibition by 1,25(OH)$_2$D$_3$ and EB 1089, 7.5×10^4 LNCaP-AI/CSS, 0.75×10^4 BPH-1, and 1.5×10^4 NRP-152 cells were seeded in 6-well plates in their corresponding medium containing 5% FBS and allowed to attach overnight. The next day, fresh media containing 1,25(OH)$_2$D$_3$ or EB 1089 (1 and 10 nM) or ethanol vehicle control (0.1% total volume) were added. After 3 days, the medium was changed and replenished. On the sixth day, cells were removed by

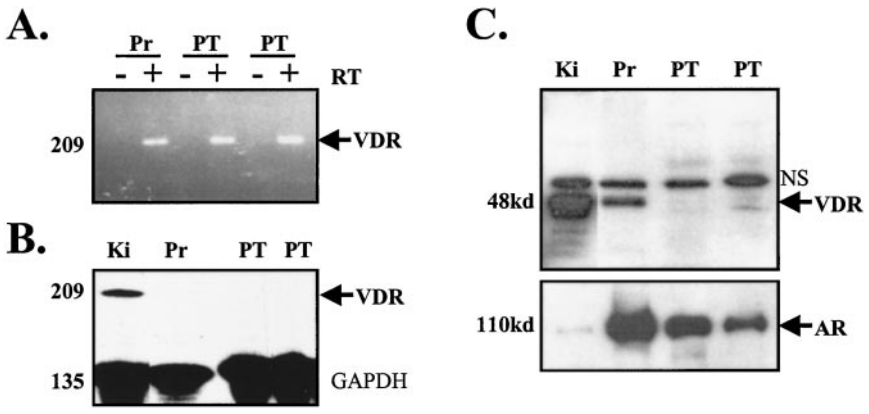

Fig. 2. Low level expression of VDR in Gγ/T-15 prostate tumors. *A*, RT-PCR of mouse VDR mRNA was performed using total RNA from mouse prostate (*Pr*) and prostate tumors (*PT*). A 209-bp product was detected in RNA samples containing reverse transcriptase (*RT*; +), but not without reverse transcriptase (*RT*; −). (B) Quantitative RPA detecting mouse VDR mRNA in kidney (*Ki*), but not in prostate (*Pr*) nor prostate tumors (*PT*). GAPDH was used as an internal RNA control. Autoradiograms were exposed to film for 7 days. The sizes of the protected fragments are 209 bp (*VDR*) and 135 bp (*GAPDH*). *C*, 10 μg of nuclear protein from mouse kidney (*Ki*), prostate (*Pr*), and prostate tumor (*PT*) were analyzed by Western blot using antibodies specific for VDR (M_r 48,000) and AR (M_r 110,000). Results showed little or no expression of VDR in prostate tumor but showed abundant expression in kidney. VDR protein was detected in prostate, despite not being detected by RPA (*B*). In contrast, there was abundant expression of AR in prostate and prostate tumor and minimal expression in kidney. *NS*, a major nonspecific band reacting with the VDR antibody. Relatively equal amounts of proteins were loaded based on Coomassie Blue staining of membranes after ECL detection. *kd*, molecular weight in thousands.

trypsin-EDTA (Life Technologies, Inc.), and viable cells were counted with a Neubauer hemacytometer. In all of the experiments, the control-treated cells reached 80–90% confluency after 6 days of growth and were presumed to be in a log-growth phase. Cell numbers in each experiment were derived from the average value of quadruplicate wells repeated three independent times and calculated as percentage of vehicle control. Statistical differences between $1,25(OH)_2D_3$- and EB 1089-treated and control cells were determined by two-tailed Student's *t* test.

Result

Localization of Tag-expressing Cells to the Basal Epithelial Layer of Transgenic Prostates. Although our previous results in the Gγ/T-15 transgenic mice suggest that the targeted prostate cells are androgen-independent (24), the location of the Tag-expressing target cells before tumor formation was not identified. To localize putative target cells, prostates without visible tumors were analyzed for Tag expression. Results showed areas of preneoplastic foci similar to high-grade PIN and dysplasia containing epithelial cells expressing Tag surrounded by normal-appearing prostate (Fig. 1). In these latter areas, isolated dispersed Tag-expressing cells were identified only in the basal epithelial layer. In proliferating areas, Tag-expressing cells were seen producing an elevation of the surface layer into and filling the prostatic lumen (Fig. 1, *C* and *D*). These results indicate that the target cells of carcinogenesis in Gγ/T-15 are located in the basal epithelial layer.

VDR Expression in Advanced Gγ/T-15 Prostate Tumors. It has previously been shown that $1,25(OH)_2D_3$ does not inhibit the proliferation of prostate cancer cells that do not express VDR (7). Although we detected VDR mRNA in Gγ/T-15 prostate tumors by RT-PCR, we were unable to detect VDR mRNA by RPA and VDR protein by Western blot analysis (Fig. 2). As positive controls, VDR mRNA was detected in mouse kidney and VDR protein was detected in normal mouse prostate and kidney. In contrast to VDR expression, abundant amounts of AR protein were detected in advanced Gγ/T-15 prostate tumors (Fig. 2*C*). These results indicate that not all steroid hormone receptors are lost during prostate tumor progression in Gγ/T-15.

Can EB 1089 Prevent or Delay Prostate Tumors in Gγ/T-15 Mice? Gγ/T-15 mice express Tag mRNA in the prostate at 11 weeks (data not shown) and start developing prostate tumors by 16 weeks of age (24). We chose three different treatment starting time points (14, 11, and 9 weeks) before tumor onset to test the ability of EB 1089 to chemoprevent or delay the onset of prostate tumors in Gγ/T-15 mice. Our results showed that EB 1089 treatment (0.5, 2, 3, 4, 5, and 10 μg/kg) starting at 14 weeks did not prevent or delay tumor onset compared with placebo-treated mice (Table 1). The percentage of mice at 24 weeks that developed prostate tumors and the average age of tumor onset were not significantly different between any of the EB 1089 treatment groups compared with placebo-treated mice. Similar results were obtained when EB 1089 treatment started at 11 weeks (0.5, 2, 3, and 4 μg/kg) and at 9 weeks (2 μg/kg; Table 1). Overall, 86% of EB 1089-treated ($n = 116$) compared with 94% of placebo-treated ($n = 31$) mice developed prostate tumors by 24 weeks of age, which indicated that EB 1089 did not prevent or delay the onset of prostate tumors in the Gγ/T-15 transgenic mice.

Can EB 1089 Slow the Growth of Primary and Metastatic Prostate Tumors in Gγ/T-15 Mice? We next sought to determine whether EB 1089-treated mice in the 14-, 11-, and 9-week groups have smaller prostate tumors compared with placebo-treated mice. Twenty-one days after first detecting a palpable mass in the urogenital region, we removed primary prostate tumors and metastases to lymph nodes, adrenal glands, and kidney and determined their wet weights. Results showed that in the 14-week group, compared with placebo-treated mice, there was a significant 30–60% reduction in the weight of primary prostate tumors using EB 1089 doses of 4, 5, and 10 μg/kg (Fig. 3*A*). There was a significant decrease in the number of metastases in mice treated with 10 mg/kg EB 1089 compared with placebo controls (0.8 *versus* 1.9 metastases per mouse; Table 2) but no differences in the sites of metastasis (lymph nodes, adrenal, and kidney) in any of the treatment groups. There was no significant difference in the weights of metastatic prostate tumors (Fig. 3*B*). As expected, there was a significant increase in serum calcium and a decrease in body weight with increasing EB 1089 doses (Fig. 3, *C* and *D*). Because mice

Table 1 Prostate tumor frequency and age of onset in EB 1089- and placebo-treated Gγ/T-15 transgenic mice

Treatment	Start (wk)[a]	No. of mice	% prostate tumor[b]	Avg. age of onset[c] (wk)
Placebo	14	12	100 (12/12)	19.4 (3.0)
EB 1089				
0.5		10	80 (8/10)	18.5 (3.2)
2		9	78 (7/9)	20.4 (2.2)
3		14	86 (12/14)	19.3 (2.4)
4		11	91 (10/11)	18.6 (3.1)
5		13	77 (10/13)	20.2 (3.0)
10		6	83 (5/6)	17.5 (2.0)
Placebo	11	10	90 (9/10)	18.9 (3.1)
EB 1089				
0.5		5	100 (5/5)	16.3 (2.3)
2		9	100 (9/9)	20.1 (3.1)
3		11	100 (12/12)	18.6 (3.2)
4		14	93 (13/14)	18.5 (3.3)
Placebo	9	9	89 (8/9)	18.1 (2.7)
EB 1089				
2		14	79 (11/14)	18.1 (2.9)

[a] Age of Gγ/T-15 mice when treatment began.
[b] Percentage of mice at 24 weeks that developed prostate tumors.
[c] Age of mice when prostate tumors were first detected by palpation. Number in the parentheses is SD. There were no significant differences in % prostate tumor and age of onset between EB 1089- and placebo-treated mice.

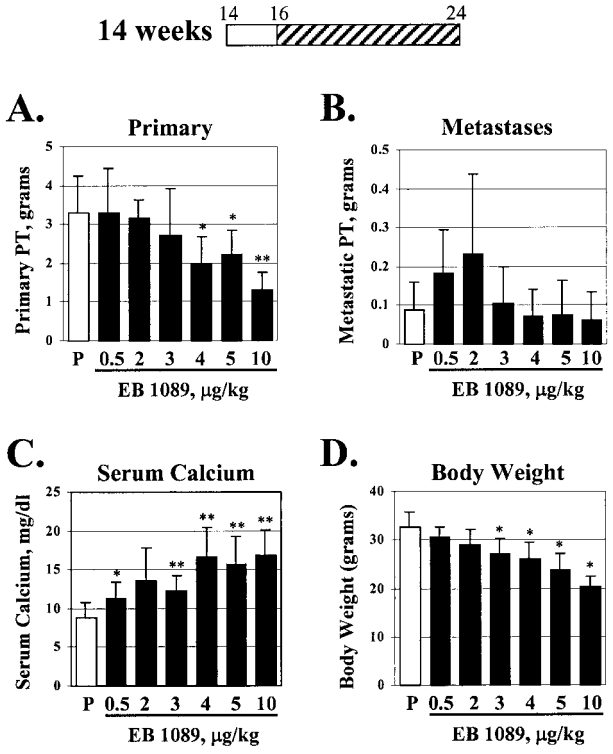

Fig. 3. High doses of EB 1089 inhibits primary prostate tumor growth in Gγ/T-15 transgenic mice. Transgenic males 14 weeks of age were treated with EB 1089 or placebo. *Bar at the top*, treatment period for the 14-week group; □, 14 to 16 weeks, the period between the start of treatment and examination of mice for tumor formation by palpation. ▨, 16 to 24 weeks, the period of tumor onsets (*16 weeks*) and the end point of the study (*24 weeks*). Average weights of primary (*A*) and metastatic (*B*) prostate tumors excised from Gγ/T-15 males treated with increasing doses of EB 1089 [0.5, 2, 3, 4, 5, and 10 μg/kg (■)] compared with the weights of prostate tumors excised from placebo-treated mice (□). Prostate tumors were allowed to grow for 21 days after the first detecting by palpation (see "Materials and Methods"). Significant difference in the primary (*A*) but not metastatic (*B*) prostate tumor weight was achieved using the 4, 5, and 10 μg/kg dose of EB 1089 (*, $P < 0.05$; **, $P < 0.005$; two-tailed Student's *t* test). Increase in serum calcium levels (mg/dl; *C*) and decrease in total body weight (grams; *D*) in Gγ/T-15 mice treated with increasing doses of EB 1089 (0.5, 2, 3, 4, 5, and 10 μg/kg) compared with placebo-treated mice. Results are expressed as means ± SD (*error bars*). *, $P < 0.05$; **, $P < 0.005$; by two-tailed Student's *t* test.

treated with EB 1089 lost body weight, we performed an analysis of covariance to determine whether the observed decrease in tumor weight could be accounted for by the decrease in overall body weight. ANOVA indicated that the decrease in tumor weight was independent of the loss in body mass ($P < 0.01$).

Because of the concern that long-term treatment with high doses of EB 1089 (>4 μg/kg) might result in hypercalcemia and loss of body weight, we treated Gγ/T-15 transgenic mice in the 11- and 9-week groups with lower doses of EB 1089. The results showed that there were no significant differences in the weights of primary and metastatic prostate tumors and in the number of metastases for all EB 1089 doses in the 11-week (0.5, 2, 3, and 4 μg/kg) and 9-week (2 μg/kg) groups (Figs. 4 and 5; Table 2). Overall, our results indicate that high doses of EB 1089 (4, 5, and 10 μg/kg) had a significant antiprostate tumor effect in the 14-week group of Gγ/T-15 transgenic mice.

Tag-expressing Prostate Cells Are Inhibited by EB 1089. Why did EB 1089 inhibit the growth of prostate tumors but not prevent or delay their occurrence? One possible explanation is that expression of Tag blocks the antiproliferative effect of EB 1089. A previous report showed that when human prostate cancer cells are transformed with Tag, but not with human papillomavirus, the result is a loss of growth inhibition by $1,25(OH)_2D_3$ (33). Preliminary experiments showed that mouse cell lines derived from Gγ/T-15 prostate tumors were growth inhibited by $1,25(OH)_2D_3$, despite expression of Tag (data not shown). To address this issue further, we compared the antiproliferative effects of $1,25(OH)_2D_3$ and EB 1089 using the Tag-expressing human prostate epithelial cell line BPH-1 (31). Our results showed that EB 1089 significantly inhibited the growth of BPH-1 cells and was more effective than $1,25(OH)_2D_3$ (Fig. 6). Thus, these results indicate that the expression of Tag does not explain the lack of chemoprevention effect of EB 1089.

EB 1089, but not $1,25(OH)_2D_3$, Inhibits Androgen-independent LNCaP-AI/CSS Cells. Another possibility for the inability of vitamin D compounds to chemoprevent prostate tumors in this model is that AIPC cells may be resistant to the antiproliferative effects of EB 1089, as they are to the antiproliferative effects of $1,25(OH)_2D_3$ (8). To address this possibility, we compared the antiproliferative effects of $1,25(OH)_2D_3$ and EB 1089 using LNCaP-AI/CSS, an androgen-independent derivative of LNCaP-FGC grown long-term in charcoal-stripped FBS (androgen-depleted conditions). Our results showed that EB 1089, but not $1,25(OH)_2D_3$, significantly inhibits the growth of LNCaP-AI/CSS cells (Fig. 6). Thus, we conclude that the inability of EB1089 to chemoprevent prostate tumors in these mice is not attributable to the androgen insensitivity of this tumor.

Prostate Basal Epithelial Cells NRP-152 Are Insensitive to the Antiproliferative Effects of EB 1089. Alternatively, it is possible that EB 1089 cannot inhibit the growth of the Tag-expressing target cells located in the basal epithelial layer (Fig. 1). To address this possibility, we used the normal rat prostate

Table 2 Number of metastases in EB 1089- and placebo-treated Gγ/T-15 transgenic mice

Treatment	Start (wk)[a]	No. of mice[b]	No. of metastases[c]
Placebo	14	9	1.89 (0.6)
EB 1089			
0.5		7	2.29 (1.1)
2		5	2.40 (0.5)
3		10	1.60 (0.5)
4		8	1.50 (1.1)
5		6	2.17 (0.8)
10		5	0.80 (0.4)[d]
Placebo	11	7	1.86 (0.4)
EB 1089			
0.5		5	2.20 (1.1)
2		6	2.00 (0.6)
3		9	1.89 (0.6)
4		12	1.67 (0.9)
Placebo	9	7	2.29 (1.3)
EB 1089			
2		10	2.00 (1.2)

[a] Age of Gγ/T-15 mice when treatment began.
[b] Gγ/T-15 mice with prostate tumors treated for 21 days with placebo or EB 1089.
[c] Number of visible metastatic lesions (lymph node, adrenal, and kidney) per mouse. Number in the parentheses is SD.
[d] Significant difference: $P < 0.005$, two-tailed Student's *t* test.

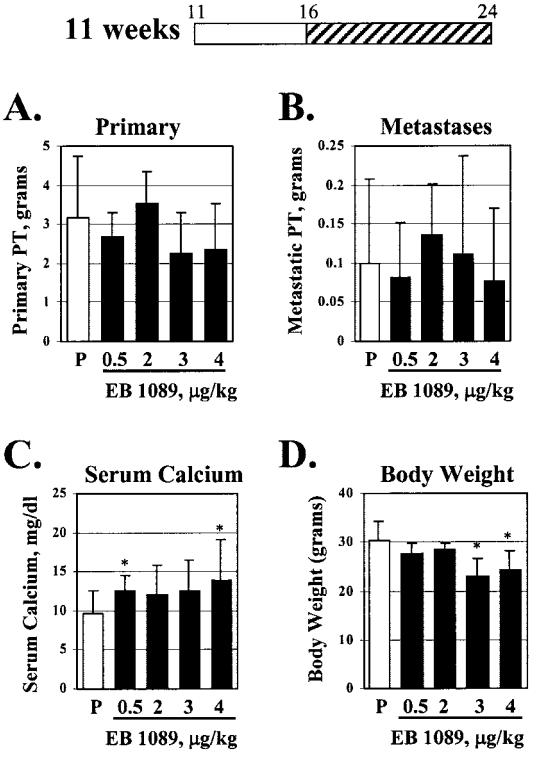

Fig. 4. Treatment of Gγ/T-15 mice with EB 1089 compared with placebo control: 11-week group. Methods are similar to the 14-week group (see Fig. 3 legend) except that treatment started at an earlier time point (11 weeks). No significant difference in the primary (*A*) and metastatic (*B*) prostate tumor weight was achieved using EB 1089 doses of 0.5, 2, 3, and 4 μg/kg (■) compared with placebo controls (□). Increase in serum calcium levels (mg/dl; *C*) and decrease in total body weight (grams; *D*) in Gγ/T-15 mice treated with increasing doses of EB 1089 (0.5, 2, 3, and 4 μg/kg) compared with placebo-treated mice. Results are expressed as means ± SD (*error bars*). (*, $P < 0.05$; **, $P < 0.005$; by two-tailed Student's *t* test).

basal epithelial cell line NRP-152, known to express VDR (32). These cells can differentiate from a basal to a luminal prostate epithelial phenotype *in vitro* and *in vivo* (34, 35). Our results showed that neither $1,25(OH)_2D_3$ nor EB 1089 (1 and 10 nM) inhibited the growth of NRP-152 cells; in fact, a small stimulation (6–16%) of cell growth was observed (Fig. 6). Thus, these results suggest that EB 1089 was not effective in chemopreventing prostate tumors in these transgenic mice because, like NRP-152 cells, the target cells of carcinogenesis are located in the basal epithelial layer.

Discussion

In this report, we showed that the Gγ/T-15 transgenic mouse model of AIPC expresses Tag to the basal epithelial layer of cells, distinguishing these mice from transgenic mouse models that express Tag to secretory luminal epithelial and neuroendocrine cells (36–42). We used the Gγ/T-15 mice to test the efficacy of the $1,25(OH)_2D_3$ analogue EB 1089 against AIPC. Our results showed that EB 1089 did not prevent or delay prostate tumor incidence. However, high doses of EB 1089 (>4 μg/kg) significantly inhibited primary prostate tumor growth, although this inhibition was accompanied by significant hypercalcemia and weight loss. Only the highest dose of EB 1089 (10 μg/kg) inhibited the number of metastases. We provide evidence suggesting that EB 1089 is ineffective in preventing or delaying primary prostate tumor onset in these mice because the target Tag-expressing epithelial cells are insensitive to the antiproliferative effects of EB 1089. Our data also suggest that low doses of EB 1089 did not inhibit prostate tumor growth because of the low expression levels of VDR.

Transgenic models of prostate cancer that use Tag have several notable properties. Prostate-specific promoters that target Tag to androgen-dependent secretory luminal epithelial cells result in tumor progression similar to that of human prostate cancer, *i.e.*, initiation as androgen-dependent and variable progression to androgen-independent disease (36–40). In contrast, targeting of Tag to mouse prostatic neuroendocrine cells results in rapid neoplastic transformation and progression to AIPC, with similarities to prostate small cell carcinoma in humans, which does not express AR (42). Although Gγ/T-15 mice express the neuroendocrine marker chromogranin A (24), the target cells are probably not neuroendocrine cells because normal Tag-expressing epithelial cells are detected before neoplasia; *i.e.*, there is a latent period before transformation (Fig. 1), and AR is expressed in advanced tumors (Fig. 2).

Advanced prostate tumors in Gγ/T-15 mice are probably not basal cell carcinomas, which are uncommon in humans (43), because they express cytokeratin 8 (Ref. 24 and data not shown) and AR (Fig. 2), common markers of luminal secretory epithelial cells and prostate cancer in humans (44). A prevailing view is that prostate stem cells are located in the basal epithelial layer and that they give rise to basal, neuroendocrine, and luminal epithelial cells during the process of cellular differentiation (45, 46). In addition, increasing evidence shows that more-aggressive metastatic AIPC express markers found in normal basal and neuroendocrine epithelial cells, suggesting a role in the origin of prostate cancer (47). More definitive experiments, *e.g.*, colocalization of Tag with a basal epithelial-specific marker, will be required to confirm that the target cells of carcinogenesis in the Gγ/T-15 mice are basal epithelial cells. Additional studies will determine the molecular changes that occur during the progression from the Tag-expressing target

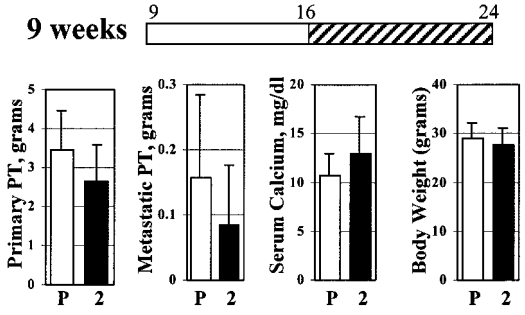

Fig. 5. Treatment of Gγ/T-15 mice with EB 1089 compared with placebo control: 9-week group. Methods are similar to the 14-week group (see Fig. 3 legend) except that treatment started at an earlier time point (*9 weeks*). No significant difference in the primary (*A*), metastatic (*B*) prostate tumor weight, serum calcium levels (*C*), and total body weight (two-tailed Student's t test) was achieved using EB 1089 dose 2 μg/kg (■) compared with placebo controls (□). Results are expressed as means ± SD (*error bars*).

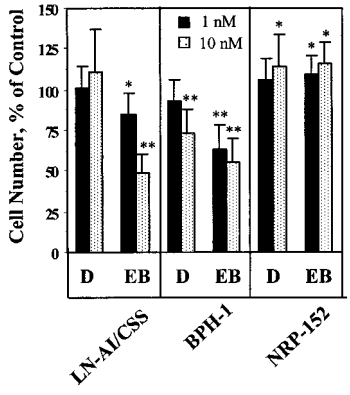

Fig. 6. EB 1089 inhibits growth of androgen-independent LNCaP and Tag-expressing BPH-1 but not of basal epithelial prostate NRP-152 cells. LNCaP-AI/CSS, BPH-1, and NRP-152 cells were treated for 6 days with 1 and 10 nM $1,25(OH)_2D_3$ (*D*) or EB 1089 (*EB*) and cell numbers expressed as % of vehicle control (see "Materials and Methods"). EB 1089 was a better inhibitor of LNCaP-AI/CSS and BPH-1 cells compared with $1,25(OH)_2D_3$. In contrast, EB 1089 and $1,25(OH)_2D_3$ treatment resulted in a small increase in NRP-152 cell numbers. *Error bars*, SD. Statistical differences between $1,25(OH)_2D_3$- and EB 1089-treated and control cells were determined by two-tailed Student's t test (*, $P < 0.05$; **, $P < 0.005$). Cell numbers from each experiment were derived from the average value of quadruplicate wells repeated three independent times.

cells to high-grade PIN and early prostate tumors in the Gγ/T-15 mice.

Our data do not support the hypothesis that expression of Tag blocks EB 1089's antiproliferative effect and, therefore, accounts for the lack of chemopreventive effect in Gγ/T-15 mice. We demonstrated that EB 1089 significantly inhibited the proliferation of the Tag-expressing BPH-1 cell line and that EB 1089 was more effective in this regard than $1,25(OH)_2D_3$ (Fig. 6). These results suggest that EB 1089 might be useful in the treatment of BPH. Additionally, our findings should encourage treatment of TRAMP mice (37, 39) with EB 1089 without the concern that Tag expression would block its antiproliferative effect. The TRAMP mice develop prostate cancer from Tag-expressing normal androgen-dependent luminal epithelial cells and progress through androgen-dependent and -independent stages of prostate tumor growth, leading to distant metastases (37, 39). Rather, our data suggest that EB 1089 had minimal effect on prostate tumor incidence in Gγ/T-15 mice because the target cells of carcinogenesis in this model were insensitive to EB 1089. Data obtained *in vitro* showed that, unlike other prostate epithelial cell types, only the rat basal epithelial cell line NRP-152 (32, 34) was insensitive to EB 1089 (Fig. 6). It is interesting that these cells have been previously shown to express VDR and to respond to $1,25(OH)_2D_3$; thus the lack of response is not caused by lack of the appropriate receptor (32, 48). It is not uncommon for $1,25(OH)_2D_3$ and its analogues to have different potencies in the same cell line (compare the lack of effect of $1,25(OH)_2D_3$ in LNCaP-AI/CSS cells in which EB 1089 was strongly antiproliferative). NRP-152 cells are considered to have stem cell properties because they can differentiate into luminal epithelial cells *in vitro* and *in vivo* (34, 35). It would be interesting to determine whether EB 1089 is more effective in preventing or delaying prostate tumors in TRAMP mice, in which secretory luminal epithelial cells are more likely to be sensitive to the antiproliferative effects of EB 1089.

Our results also suggest that the minimal antiproliferative effect of EB 1089 at low doses in Gγ/T-15 mice may be attributable to low levels of VDR protein expression (Fig. 2). The effects of $1,25(OH)_2D_3$ on growth and differentiation of prostate cancer cells are generally thought to require the presence of active VDR (7). Recent results demonstrate high variability in the expression of VDR in secretory luminal epithelial cells present in normal human prostates (49). Given the various sensitivities to growth inhibition by $1,25(OH)_2D_3$ in prostate cancer cell lines and the variable expression of VDR in normal human prostate, such variability is likely to exist in human prostate cancers. It is noteworthy that EB 1089 was effective in suppressing the growth of androgen-insensitive prostate cancer cells in which $1,25(OH)_2D_3$ had little or no effect (*e.g.*, LNCaP-AI/CSS and BPH-1; Fig. 6; Ref. 50). These findings support the use of EB 1089 in AIPC. A recent clinical trial indicates that very high doses of $1,25(OH)_2D_3$ can be administered p.o. without inducing hypercalcemia by giving the drug in pulses (51). This approach may similarly permit the administration of higher doses of EB 1089, which is also administered p.o.

The mechanisms of how high doses of EB 1089 inhibit the growth of primary prostate tumors in the Gγ/T-15 mice are currently unknown. However, it is reasonable to expect that these mechanisms are similar to those by which $1,25(OH)_2D_3$ inhibits tumor growth, *e.g.*, induction of cyclin-dependent kinase inhibitor p21 and G_1-G_0 cell cycle arrest (7). Because of the large size of the primary prostate tumors, there were extensive areas of necrosis, making it difficult to identify histological differences. This question may be resolved in the future by treating transgenic males with EB 1089 (10 μg/kg) for a short period of time to obtain smaller prostate tumors and histological sections with smaller areas of necrosis.

A high dose of EB 1089 (10 μg/kg) was required to inhibit the number of metastases in the Gγ/T-15 mice (Table 2). This is in agreement with the antimetastasis effect of EB 1089 in the MATLyLu model of prostate cancer (16). The differences in our results and the more striking effect on metastasis in the MATLyLu model may be attributed to the sites of tumor growth, *i.e.*, in the natural prostate microenvironment in Gγ/T-15 mice compared with the s.c. microenvironment in MATLyLu rats. It may be easier for tumor cells to migrate from the s.c. microenvironment rather than invade through the prostate stroma into the vasculature.

In summary, we suggest that EB 1089 does not chemoprevent prostate tumors in Gγ/T-15 transgenic mice primarily because the target cells are insensitive to its antiproliferative

effect. Low levels of VDR expression in Gγ/T-15 prostate tumors may also contribute to a lack of growth-inhibitory effect of EB 1089 at low doses. However, high doses of EB 1089 had a significant antiprostate tumor effect in Gγ/T-15 mice. To our knowledge, this is the first report of testing the efficacy of a vitamin D analogue in a transgenic mouse model of prostate cancer. These data underscore the fact that chemoprevention and chemotherapy involve different biological processes. We conclude that the Gγ/T-15 transgenic mice provide an effective preclinical animal model system of AIPC in which to test novel therapies (52). The superiority of EB 1089 over $1,25(OH)_2D_3$ in inhibiting the growth of AIPC *in vitro* suggests that this analogue may be useful clinically, particularly if the problem of hypercalcemia can be overcome.

Acknowledgments

We thank the anonymous reviewers for their thoughtful suggestions; Alicia De Las Pozas for excellent technical assistance; Dr. Kerry Burnstein for critical comments; Drs. David Danielpour (Case Western Reserve University, Cleveland, OH) and Simon Hayward (Vanderbilt University School of Medicine, Nashville, TN) for prostate cell lines; and Dr. Carolyn Cray () for serum calcium measurements.

References

1. Greenlee, R. T., Murray, T., and Thun, M. Cancer Statistics, 2001. CA Cancer J. Clin., *51:* 15–36, 2001.

2. Pilat, M. J., Kamradt, J. M., and Pienta, K. J. Hormone resistance in prostate cancer. Cancer Metastasis Rev., *17:* 373–381, 1999.

3. Schwartz, G. G., and Hulka, B. S. Is vitamin D deficiency a risk factor for prostate cancer? (Hypothesis). Anticancer Res., *10:* 1307–1311, 1990.

4. Hanchette, C. L., and Schwartz, G. G. Geographic patterns of prostate cancer mortality: evidence for a protective effect of ultraviolet radiation. Cancer (Phila.), *70:* 2861–2869, 1992.

5. Schwartz, G. G. Prostate cancer and vitamin D: from concept to clinic. A 10-year update. *In:* A. W., Norman, R. Bouillon, and M. Thomasset (eds.), Vitamin D Endocrine System, pp. 445–452. Berkeley, CA: University of California Press, 2000.

6. Ahonen, M. H., Tenkanen, L., Teppo, L., Hakama, M., and Tuohimaa, P. Prostate cancer risk and prediagnostic serum 25-hydroxyvitamin D levels (Finland). Cancer Causes Control, *11:* 847–852, 2000.

7. Miller, G. J. Vitamin D and prostate cancer: biological interactions and clinical potentials. Cancer Metastasis Rev., *17:* 353–360, 1999.

8. Zhuang, S-H, Schwartz, G. G., Cameron, D., and Burnstein, K. L. Vitamin D receptor content and transcriptional activity do not fully predict antiproliferative effects of vitamin D in human prostate cancer cell lines. Mol. Cell. Endocrinol., *126:* 83–90, 1997.

9. Osborn, J. L., Schwartz, G. G., Smith, D. C., Bahnson, R., Day, R., and Trump, D. L. Phase II trial of oral 1,25-dihydroxyvitamin D (calcitriol) in hormone refractory prostate cancer. Urol. Oncol., *1:* 195–198, 1995.

10. Gross, C., Stamey, T., Hancock, S., and Feldman, D. Treatment of early recurrent prostate cancer with 1,25-dihydroxyvitamin D_3 (calcitriol). J. Urol., *159:* 2035–2040, 1998.

11. Mathiasen, I. S., Colston, K. W., and Binderup, L. EB 1089, a novel vitamin D analogue, has strong antiproliferative and differentiation inducing effects on cancer cells. J. Steroid Biochem. Mol. Biol., *46:* 365–371, 1993.

12. De Vos, S., Holden, S., Heber, D., Elstner, E., Binderup, L., Uskokovic, M., Rude, B., Chen, D. L., Le, J., Cho, S. K., and Koeffler, H. P. Effects of potent vitamin D_3 analogs on clonal proliferation of human prostate cancer cell lines. Prostate, *31:* 77–83, 1997.

13. Wang, X., Chen, X., Akhter, J., and Morris, D. L. The *in vitro* effect of vitamin D_3 analogue EB-1089 on a human prostate cancer cell line (PC-3). Br. J. Urol., *80:* 260–262, 1997.

14. Skowronski, R. J., Peehl, D. M., and Feldman, D. Actions of vitamin D_3 analogs on human prostate cancer cell lines: comparison with 1,25-dihydroxyvitamin D_3. Endocrinology, *136:* 20–26, 1995.

15. Blutt, S. E., Polek, T. C., Stewart, L. V., Kattan, M. W., and Weigel, N. L. A calcitriol analogue. EB 1089, inhibits the growth of LNCaP tumors in nude mice. Cancer Res., *60:* 779–782, 2000.

16. Lokeshwar, B. L., Schwartz, G. G., Selzer, M. G., Burnstein, K. L., Zhuang, S-H. Block, N. L, Binderup, L. Inhibition of prostate cancer metastasis in vivo: a comparison of 1,25-dihydroxyvitamin D (calcitriol) and EB 1089. Cancer Epidemiol. Biomark. Prev., *8:* 241–248, 1999.

17. Xue, L., Lipkin, M., Newmark, H., and Wang, J. Influence of dietary calcium and vitamin D on diet-induced epithelial cell hyperproliferation in mice. J. Natl. Cancer Inst. (Bethesda), *91:* 176–181, 1999.

18. Schwartz, G. G., Wang, M. H., Zang, M., Singh, R. K., and Siegal, G. P. 1α,25-Dihydroxyvitamin D (calcitriol) inhibits the invasiveness of human prostate cancer cells. Cancer Epidemiol. Biomarkers Prev., *6:* 727–732, 1997.

19. Lucia, M. S., Bostwick, D. G., Bosland, M., Cockett, A. T., Knapp, D. W., Leav, I., Pollard, M., Rinker-Schaeffer, C., Shirai, T., and Watkins, B. A. Workgroup I: rodent models of prostate cancer. Prostate, *36:* 49–55, 1998.

20. Green, J. E., Greenberg, N. M., Ashendel, C. L., Barrett, J. C., Boone, C., Getzenberg, R. H., Henkin, J., Matusik, R., Janus, T. J., and Scher, H. I. Workgroup 3: transgenic and reconstitution models of prostate cancer. Prostate, *36:* 59–63, 1998.

21. Lucia, M. S., Anzano, M. A., Slayter, M. V., Anver, M. R., Green, D. M., Shrader, M. W., Logsdon, D. L., Driver, C. L., Brown, C. C., Peer, C. W., Roberts, A. B., and Sporn, M. B. Chemopreventive activity of tamoxifen, *N*-(4-hydroxyphenyl) retinamide, and the vitamin D analogue Ro24-5531 for androgen-promoted carcinomas of the rat seminal vesicle and prostate. Cancer Res. 55: 5621–5627, 1995.

22. Sharma, P., and Schreiber-Agus, N. Mouse models of prostate cancer. Oncogene., *18:* 5349–5355, 1999.

23. Perez-Stable, C., Altman, N. H., Brown, J., Harbison, M. Cray, C., and Roos, B. A. Prostate, adrenocortical, and brown adipose tumors in fetal globin/T antigen transgenic mice. Lab. Investig., *74:* 363–373, 1996.

24. Perez-Stable, C., Altman, N., Mehta, P., Deftos, L., and Roos, B. A. Prostate cancer progression, metastasis, and gene expression in transgenic mice. Cancer Res., 57: 900–906, 1997.

25. Perez-Stable, C. Distinct negative regulatory mechanisms involved in the repression of human embryonic ϵ- and fetal Gγ-globin genes in transgenic mice. J. Biol. Chem., *269:* 33109–33115, 1994.

26. Sepulveda, A. R., Finegold, M. J., Smith, B., Slagle, B. L., DeMayo, J. L., Shen, R. F., Woo, S. L., and Butel, J. S. Development of a transgenic mouse system for the analysis of stages in liver carcinogenesis using tissue-specific expression of SV40 large T-antigen controlled by regulatory elements of the human α-1-antitrypsin gene. Cancer Res. *49:* 6108–6117, 1989.

27. Auffray, C., and Rougeon, F. Purification of mouse immunoglobulin heavy chain messenger RNAs from total myeloma tumor DNA. Eur. J. Biochem., *107:* 303–314, 1980.

28. Kamei Y, Kawada T, Fukuwatari T, Ono T, Kato S, and Sugimoto E. Cloning and sequencing of the gene encoding the mouse vitamin D receptor. Gene, *152:* 281–282, 1995.

29. Dent, C. L., and Latchman, D. S. The DNA mobility shift assay. *In:* D. S. Latchman (ed.), Transcription Factors: A Practical Approach, pp. 1–26. New York: Oxford University Press, 1993.

30. Horoszewicz, J. S., Leong, S. S., Kawinski, E., Kerr, J. P., Rosenthal, H., Chu, T. M., Mirand, E. A., and Murphy, G. P. LNCaP model of human prostatic carcinoma. Cancer Res., 43: 1809–1818, 1983.

31. Hayward, S. W., Dahiya, R., Cunha, G. R., Bartek, J., Deshpande, N., and Narayan, P. Establishment and characterization of an immortalized but non-transformed human prostate epithelial cell line: BPH-1. In Vitro Cell. Dev. Biol., *31A:* 14–24, 1995.

32. Danielpour, D., Kadomatsu, K., Anzano, M. A., Smith, J. M., and Sporn, M. B. Development and characterization of nontumorigenic and tumorigenic epithelial cell lines from rat dorsal-lateral prostate. Cancer Res., 54: 3413–3421, 1994.

33. Gross, C., Skowronski, R. J., Plymate, S. R., Rhim, J. S., Peehl, D. M., and Feldman, D. Simian virus 40-, but not human papillomavirus-, transformation of prostate epithelial cells results in loss of growth-inhibition by 1,25-dihydroxyvitamin D_3. Int. J. Oncol., *8:* 41–47, 1996.

34. Danielpour, D. Transdifferentiation of NRP-152 rat prostatic basal epithelial cells toward a luminal phenotype: regulation by glucocorticoid, insulin-like growth factor-I and transforming growth factor-β. J. Cell Sci., *112:* 169–179, 1999.

35. Hayward, S. W., Haughney, P. C., Lopes, E. S., Danielpour, D., and Cunha, G. R. The rat prostatic epithelial cell line NRP-152 can differentiate *in vivo* in response to its stromal environment. Prostate, *39:* 205–212, 1999.

36. Maroulakou, I. G., Anver, M., Garrett, L., and Green, J. E. Prostate and mammary adenocarcinoma in transgenic mice carrying a rat C3(1) simian virus 40 large tumor antigen fusion gene. Proc. Natl. Acad. Sci. USA, *91:* 11236–11240, 1994.

37. Greenberg, N. M., DeMayo, F., Finegold, M. J., Medina, D., Tilley, W. D., Aspinall, J. O., Cunha, G. R., Donjacour, A. A., Matusik, R. J., and Rosen, J. M.

Prostate cancer in a transgenic mouse. Proc. Natl. Acad. Sci. USA, *92:* 3439–3443, 1995.

38. Kasper, S., Sheppard, P. C., Yan, Y., Pettigrew, N., Borowsky, A. D., Prins, G. S., Dodd, J. G., Duckworth, M. L., and Matusik, R, J. Developmental progression and androgen-dependence of prostate tumors in probasin-large T antigen transgenic mice: a model for prostate cancer. Lab. Investig., *78:* 319–333, 1998.

39. Gingrich, J. R., Barrios, R. J., Kattan, M. W., Nahm, H. S., Finegold, M. J., and Greenberg, N. M. Androgen-independent prostate cancer progression in the TRAMP model. Cancer Res., *57:* 4687–4691, 1997.

40. Masumori, N., Thomas, T. Z., Chaurand, P., Case, T., Paul, M., Kasper, S., Caprioli, R. M., Tsukamoto, T., Shappell, S. B., and Matusik, R. J. A probasin-large T antigen transgenic mouse line develops prostate adenocarcinoma and neuroendocrine carcinoma with metastatic potential. Cancer Res., *61:* 2239–2249, 2001.

41. Skalnik, D. G., Dorfman, D. M., Williams, D. A., and Orkin, S. H. Restriction of neuroblastoma to the prostate gland in transgenic mice. Mol. Cell. Biol., *11:* 4518–4527, 1991.

42. Garabedian, E. M., Humphrey, P. A., and Gordon, J. I. A transgenic mouse model of metastatic prostate cancer originating from neuroendocrine cells. Proc. Natl. Acad. Sci. USA, *95:* 15382–15387, 1998.

43. Denholm, S. W., Webb, J. N., Howard, G. C., and Chisholm, G. D. Basaloid carcinoma of the prostate gland: histogenesis and review of the literature. Histopathology (Oxf.), *20:* 151–155, 1992.

44. Mehta, P. P., Perez-Stable, C., Roos, B. A., and Nadji, M. Identification, characterization and differentiation of human prostate cells. *In:* R. S. Tuan and C. W. Lo (eds.), pp. 317–335. Methods in Molecular Biology: Developmental Biology Protocols. Totowa, NJ: Humana Press Inc., 2000.

45. Isaacs, J. T., and Coffey, D. S. Etiology and disease process of benign prostatic hyperplasia. Prostate Suppl., *2:* 33–50, 1989.

46. Bonkhoff, H., and Remberger, K. Differentiation pathways and histogenetic aspects of normal and abnormal prostatic growth: a stem cell model. Prostate, *28:* 98–106, 1996.

47. Bui, M., and Reiter, R. E. Stem cell genes in androgen-independent prostate cancer. Cancer Metastasis Rev., *17:* 391–399, 1999.

48. Danielpour, D. Induction of transforming growth factor-β autocrine activity by all-*trans*-retinoic acid and 1a,25-dihydroxyvitamin D_3 in NRP-152 rat prostatic epithelial cells. J. Cell Physiol., *166:* 231–239, 1996.

49. Kivineva, M., Blauer, M., Syvala, H., Tammela, T., and Tuohimaa, P. Localization of 1,25-dihydroxyvitamin D_3 receptor (VDR) expression in human prostate. J. Steroid Biochem. Mol. Biol., *66:* 121–127, 1998.

50. Hansen, C. M., Binderup, L., Hamberg, K. J., Carlberg, C. Vitamin D and cancer: effects of $1,25(OH)_2D_3$ and its analogs on growth control and tumorigenesis. Front. Biosci., *6:* D820–D848, 2001.

51. Beer, T. M., Munar, M., and Henner, W. D. A Phase I trial of pulse calcitriol in patients with refractory malignancies: pulse dosing permits substantial dose escalation. Cancer (Phila.), *91:* 2431–2439, 2001.

52. Qadan, L. R., Perez-Stable, C. M., Anderson, C. D'Ippolito, G., Herron, A., Howard, G. A., and Roos, B. A. 2-Methoxyestradiol induces G_2/M arrest and apoptosis in prostate cancer. Biochem. Biophys. Res. Comm., *285:* 1259–1266, 2001.

The Gγ/T-15 Transgenic Mouse Model of Androgen-independent Prostate Cancer: Target Cells of Carcinogenesis and the Effect of the Vitamin D Analogue EB 1089

Carlos M. Perez-Stable, Gary G. Schwartz, Adan Farinas, et al.

Cancer Epidemiol Biomarkers Prev 2002;11:555-563.